

## Chapter 2

# Dynamics of Rigid Clusters of Charged Particles

As the next level of complexity beyond the dynamics of a single particle, we consider rigid clusters of such particles. In this chapter, we consider the cluster to already be formed, with particles rigidly bound together by either mechanical, chemical or electromagnetic bonds. Investigation of the evolution of such clusters from loose, free-flowing, particulates will be discussed later in the monograph. Of particular interest is to compare and contrast the differences in the dynamics of a cluster of charged particles and that of a (hypothetical) single charged particle (with the same overall charge) whose motion is governed by

$$m\dot{\mathbf{v}} = q(\mathbf{E}^{ext} + \mathbf{v} \times \mathbf{B}^{ext}), \quad (2.1)$$

where  $m$  is the mass of the particle,  $\mathbf{v}$  is the particle velocity,  $\mathbf{E}^{ext} = (E_1^{ext}, E_2^{ext}, E_3^{ext})$  is the external electric field and  $\mathbf{B}^{ext} = (B_1^{ext}, B_2^{ext}, B_3^{ext})$  is the external magnetic field.

*Remark* Such clusters possess unique dynamics that are important in order to understand and fully control relevant industrial processes (see, for example, Luo and Dornfeld [14–17], Arbelaez et al. [1, 2], Ciampini et al. [3, 4], Gomes-Ferreira et al. [10], Ghobeity et al. [7, 8] and Zohdi [27–45]).<sup>1</sup>

### 2.1 Dynamics of Charged Clusters

Following an approach found in Zohdi [44], consider a collection of rigidly-bonded particles,  $i = 1, 2, \dots, N_c$ , in a cluster. The individual particle dynamics are described by (which leads to a coupled system)

---

<sup>1</sup> For a review of the effects of clusters on the macroscale material properties of solids that contain them, see Torquato [25], as well as Ghosh et al. [9] for domain partitioning methods that are capable of handling materials with general nonuniform microstructure. For a review of novel approaches of multiscale methods that bridge scales with applications to nanotechnology, see Fish [5].

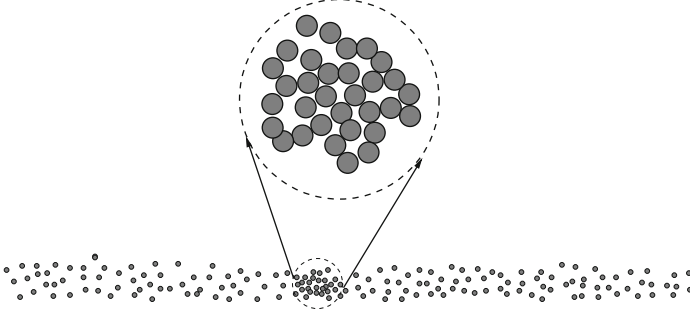


**Fig. 2.1** Agglomeration of material (formation of a cluster) within a flow of particulates (Zohdi [44])

$$m_i \ddot{\mathbf{r}}_i = \underbrace{\Psi_i^{tot}}_{\text{total forces}} = \underbrace{\Psi_i^{int}}_{\text{internal}} + \underbrace{\Psi_i^{ext}}_{\text{external}} = \underbrace{\Psi_i^{int} + q_i(E^{ext} + \mathbf{v}_i \times \mathbf{B}^{ext})}_{\Psi_i^{ext}}, \quad (2.2)$$

where  $\mathbf{r}_i$  is the position vector of the  $i$ th particle,  $m_i$  is the mass of a single particle and  $\Psi_i^{tot}$  is the sum of the forces acting on the  $i$ th particle, due to other particles in the system (“internal” particle-to-particle near-fields, bonding forces, etc.,  $\Psi_i^{int}$ ) and due to the external electric and magnetic fields ( $\Psi_i^{ext}$ ) (Fig. 2.1).

*Remarks* Although the exact nature of particle-to-particle interaction is not important in the present (overall rigid motion) analysis (it will be later) since the corresponding forces are internal to the system, in passing, we mention that there are a variety of possible interparticle representations for loose, free-flowing, charged particles. We again refer the reader to Frenklach and Carmer [6] as well as to Haile [11], Hase [12], Schlick [22], Rapaport [19], Torquato [26], Rechtsman et al. [20, 21] and Zohdi [27–45] for overviews of the various representations for particle interaction, for example, those based on the familiar Mie, Lennard–Jones, and Morse potentials (see Moelwyn-Hughes [18] for reviews). Also, three-body terms can be introduced directly into the interparticle interaction (Stillinger [23]) or via term-wise modifications to the two-body representations ( Tersoff [24]).

### 2.1.1 Group Dynamics of a Rigidly Bound Collection of Particles

When we consider a collection of particles that are bound together as a rigid body, the exact nature of the internal particle-to-particle interaction is irrelevant to the overall system dynamics since the internal forces in the system are equal in magnitude and opposite in direction, leading to

$$\sum_{i=1}^{N_c} (\Psi_i^{ext} + \Psi_i^{int}) = \sum_{i=1}^{N_c} \Psi_i^{ext} + \underbrace{\sum_{i=1}^{N_c} \Psi_i^{int}}_{=0} = \sum_{i=1}^{N_c} \Psi_i^{ext} \stackrel{\text{def}}{=} \Psi^{EXT}, \quad (2.3)$$

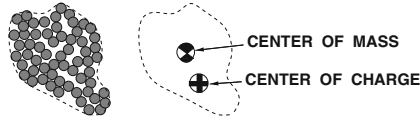


**Fig. 2.2** A collection of charged particles that are rigidly bonded together. The nature of the particle-to-particle bonding (mechanical, electronic, chemical, etc.) is irrelevant in the present analysis. The mass center and “charge” center will generally not coincide. This difference will lead to a variation in the dynamics of the center-of-mass of a cluster relative to a single charged particle of equal mass and charge, strongly influenced by the equation of overall balance of angular momentum (Zohdi [44])

where  $\Psi^{EXT}$  is the overall external force acting on the cluster and  $N_c$  are the number of particles in the cluster (Fig. 2.2). The position vector of the center of mass of the system is given by

$$\mathbf{r}_{cm} \stackrel{\text{def}}{=} \frac{\sum_{i=1}^{N_c} m_i \mathbf{r}_i}{\sum_{i=1}^{N_c} m_i} = \frac{1}{\mathcal{M}} \sum_{i=1}^{N_c} m_i \mathbf{r}_i, \quad (2.4)$$

where  $\mathcal{M}$  is the total system mass. A decomposition of the position vector for particle  $i$ , of the form  $\mathbf{r}_i = \mathbf{r}_{cm} + \mathbf{r}_{cm \rightarrow i}$ , allows the linear momentum of the system of particles ( $\mathbf{G}$ ) to be written as

$$\sum_{i=1}^{N_c} \underbrace{m_i \dot{\mathbf{r}}_i}_{\mathbf{G}_i} = \sum_{i=1}^{N_c} m_i (\dot{\mathbf{r}}_{cm} + \dot{\mathbf{r}}_{cm \rightarrow i}) = \sum_{i=1}^{N_c} m_i \dot{\mathbf{r}}_{cm} = \dot{\mathbf{r}}_{cm} \sum_{i=1}^{N_c} m_i = \mathcal{M} \dot{\mathbf{r}}_{cm} \stackrel{\text{def}}{=} \mathbf{G}_{cm} \quad (2.5)$$

since  $\sum_{i=1}^{N_c} m_i \dot{\mathbf{r}}_{cm \rightarrow i} = \mathbf{0}$ . Furthermore,  $\dot{\mathbf{G}}_{cm} = \mathcal{M} \ddot{\mathbf{r}}_{cm}$ , and thus

$$\dot{\mathbf{G}}_{cm} = \mathcal{M} \ddot{\mathbf{r}}_{cm} = \sum_{i=1}^{N_c} \psi_i^{ext} = \sum_{i=1}^{N_c} q_i (\mathbf{E}^{ext} + \mathbf{v}_i \times \mathbf{B}^{ext}) \stackrel{\text{def}}{=} \Psi^{EXT}. \quad (2.6)$$

The angular momentum relative to the center of mass can be written as (utilizing  $\dot{\mathbf{r}}_i = \mathbf{v}_i = \mathbf{v}_{cm} + \mathbf{v}_{cm \rightarrow i}$ )

$$\sum_{i=1}^{N_c} = \mathbf{H}_{cm \rightarrow i} = \sum_{i=1}^{N_c} (\mathbf{r}_{cm \rightarrow i} \times m_i \mathbf{v}_{cm \rightarrow i}) = \sum_{i=1}^{N_c} (\mathbf{r}_{cm \rightarrow i} \times m_i (\mathbf{v}_i - \mathbf{v}_{cm})) \quad (2.7)$$

$$= \sum_{i=1}^{N_c} (m_i \mathbf{r}_{cm \rightarrow i} \times \mathbf{v}_i) - \left( \underbrace{\sum_{i=1}^{N_c} m_i \mathbf{r}_{cm \rightarrow i}}_{=0} \right) \times \mathbf{v}_{cm} = \mathbf{H}_{cm} \quad (2.8)$$

for a rigid body. Since  $\mathbf{v}_{cm \rightarrow i} = \boldsymbol{\omega} \times \mathbf{r}_{cm \rightarrow i}$ ,

$$\mathbf{H}_{cm} = \sum_{i=1}^{N_c} \mathbf{H}_{cm \rightarrow i} = \sum_{i=1}^{N_c} m_i (\mathbf{r}_{cm \rightarrow i} \times \mathbf{v}_{cm \rightarrow i}) = \sum_{i=1}^{N_c} m_i (\mathbf{r}_{cm \rightarrow i} \times (\boldsymbol{\omega} \times \mathbf{r}_{cm \rightarrow i})). \quad (2.9)$$

Decomposing the relative position vector into its components

$$\mathbf{r}_{cm \rightarrow i} = \mathbf{r}_i - \mathbf{r}_{cm} = \hat{x}_{i1} \mathbf{e}_1 + \hat{x}_{i2} \mathbf{e}_2 + \hat{x}_{i3} \mathbf{e}_3, \quad (2.10)$$

where  $\hat{x}_{i1}$ ,  $\hat{x}_{i2}$  and  $\hat{x}_{i3}$  are the coordinates of the mass points measured *relative to the center of mass*, and expanding the angular momentum expression, yields

$$H_1 = \omega_1 \sum_{i=1}^{N_c} (\hat{x}_{i2}^2 + \hat{x}_{i3}^2) m_i - \omega_2 \sum_{i=1}^{N_c} \hat{x}_{i1} \hat{x}_{i2} m_i - \omega_3 \sum_{i=1}^{N_c} \hat{x}_{i1} \hat{x}_{i3} m_i \quad (2.11)$$

$$H_2 = -\omega_1 \sum_{i=1}^{N_c} \hat{x}_{i1} \hat{x}_{i2} m_i + \omega_2 \sum_{i=1}^{N_c} (\hat{x}_{i1}^2 + \hat{x}_{i3}^2) m_i - \omega_3 \sum_{i=1}^{N_c} \hat{x}_{i2} \hat{x}_{i3} m_i \quad (2.12)$$

and

$$H_3 = -\omega_1 \sum_{i=1}^{N_c} \hat{x}_{i1} \hat{x}_{i3} m_i - \omega_2 \sum_{i=1}^{N_c} \hat{x}_{i2} \hat{x}_{i3} m_i + \omega_3 \sum_{i=1}^{N_c} (\hat{x}_{i1}^2 + \hat{x}_{i2}^2) m_i, \quad (2.13)$$

which can be concisely written as

$$\mathbf{H}_{cm} = \bar{\mathcal{I}} \cdot \boldsymbol{\omega}, \quad (2.14)$$

where we define the moments of inertia with respect to the center of mass

$$\bar{\mathcal{I}}_{11} = \sum_{i=1}^{N_c} (\hat{x}_{i2}^2 + \hat{x}_{i3}^2) m_i, \quad \bar{\mathcal{I}}_{22} = \sum_{i=1}^{N_c} (\hat{x}_{i1}^2 + \hat{x}_{i3}^2) m_i, \quad \bar{\mathcal{I}}_{33} = \sum_{i=1}^{N_c} (\hat{x}_{i1}^2 + \hat{x}_{i2}^2) m_i, \quad (2.15)$$

$$\bar{\mathcal{I}}_{12} = \bar{\mathcal{I}}_{21} = - \sum_{i=1}^{N_c} \hat{x}_{i1} \hat{x}_{i2} m_i, \quad \bar{\mathcal{I}}_{23} = \bar{\mathcal{I}}_{32} = - \sum_{i=1}^{N_c} \hat{x}_{i2} \hat{x}_{i3} m_i,$$

$$\bar{\mathcal{I}}_{13} = \bar{\mathcal{I}}_{31} = - \sum_{i=1}^{N_c} \hat{x}_{i1} \hat{x}_{i3} m_i, \quad (2.16)$$

or explicitly

$$\bar{\mathcal{I}} = \begin{bmatrix} \bar{\mathcal{I}}_{11} & \bar{\mathcal{I}}_{12} & \bar{\mathcal{I}}_{13} \\ \bar{\mathcal{I}}_{21} & \bar{\mathcal{I}}_{22} & \bar{\mathcal{I}}_{23} \\ \bar{\mathcal{I}}_{31} & \bar{\mathcal{I}}_{32} & \bar{\mathcal{I}}_{33} \end{bmatrix}. \quad (2.17)$$

The particles' own inertia contribution about their respective mass-centers to the overall moment of inertia of the agglomerated body can be described by the Huygens–Steiner (generalized “parallel axis” theorem) formula ( $p, s = 1, 2, 3$ )

$$\bar{\mathcal{I}}_{ps} = \sum_{i=1}^{N_c} \left( \bar{\mathcal{I}}_{ps}^i + m_i (|\mathbf{r}_i - \mathbf{r}_{cm}|^2 \delta_{ps} - \hat{x}_{ip} \hat{x}_{is}) \right). \quad (2.18)$$

For a spherical particle,  $\bar{\mathcal{I}}_{pp}^i = \frac{2}{5} m_i R_i^2$ , and for  $p \neq s$ ,  $\bar{\mathcal{I}}_{ps}^i = 0$  (no products of inertia),  $R_i$  being the particle radius.<sup>2</sup> Finally, for the derivative of the angular momentum, utilizing  $\dot{\mathbf{r}}_i = \mathbf{a}_i = \mathbf{a}_{cm} + \mathbf{a}_{cm \rightarrow i}$ , we obtain

$$\dot{\mathbf{H}}_{cm}^{rel} = \sum_{i=1}^{N_c} (\mathbf{r}_{cm \rightarrow i} \times m_i \mathbf{a}_{cm \rightarrow i}) = \sum_{i=1}^{N_c} (\mathbf{r}_{cm \rightarrow i} \times m_i (\mathbf{a}_i - \mathbf{a}_{cm})) \quad (2.19)$$

$$= \sum_{i=1}^{N_c} (m_i \mathbf{r}_{cm \rightarrow i} \times \mathbf{a}_i) - \underbrace{\left( \sum_{i=1}^{N_c} m_i \mathbf{r}_{cm \rightarrow i} \right) \times \mathbf{a}_{cm}}_{=0} = \dot{\mathbf{H}}_{cm}, \quad (2.20)$$

and consequently

$$\dot{\mathbf{H}}_{cm} = \frac{d(\bar{\mathcal{I}} \cdot \boldsymbol{\omega})}{dt} = \sum_{i=1}^{N_c} \mathbf{r}_{cm \rightarrow i} \times \boldsymbol{\Psi}_i^{ext} = \sum_{i=1}^{N_c} \mathbf{r}_{cm \rightarrow i} \times q_i (\mathbf{E}^{ext} + \mathbf{v}_i \times \mathbf{B}^{ext}) \stackrel{\text{def}}{=} \mathbf{M}_{cm}^{EXT}, \quad (2.21)$$

where  $\mathbf{M}_{cm}^{EXT}$  is the total external moment about the center of mass.

## 2.2 Decomposition of the Electromagnetic Contributions

Consider a rigid cluster of charged particles with angular velocity  $\boldsymbol{\omega}$  and center of mass velocity  $\mathbf{v}_{cm}$ .

### 2.2.1 The Overall Forces and Moments

The velocity of any point on the body can be represented by

$$\mathbf{v}_i = \mathbf{v}_{cm} + \boldsymbol{\omega} \times \mathbf{r}_{cm \rightarrow i}, \quad (2.22)$$

---

<sup>2</sup> If the particles are sufficiently small, each particle's own moment inertia (about its own center) is insignificant, leading to  $\bar{\mathcal{I}}_{ps} = \sum_{i=1}^{N_c} m_i (|\mathbf{r}_i - \mathbf{r}_{cm}|^2 \delta_{ps} - \hat{x}_{ip} \hat{x}_{is})$ .

and the overall external electromagnetic force  $\Psi^{EXT} = \sum_{i=1}^{N_c} q_i (\mathbf{E}^{ext} + \mathbf{v} \times \mathbf{B}^{ext})$  can be decomposed into the following parts

$$\begin{aligned} \Psi^{EXT} &= \underbrace{\sum_{i=1}^{N_c} q_i \mathbf{E}^{ext}}_{\text{electrical contribution}} + \underbrace{\sum_{i=1}^{N_c} q_i (\mathbf{v}_{cm} \times \mathbf{B}^{ext})}_{\text{linear velocity contribution}} + \underbrace{\sum_{i=1}^{N_c} q_i ((\boldsymbol{\omega} \times \mathbf{r}_{cm \rightarrow i}) \times \mathbf{B}^{ext})}_{\text{angular velocity contribution}} \\ &= \mathbf{E}^{ext} \left( \sum_{i=1}^{N_c} q_i \right) + \mathbf{v}_{cm} \times \mathbf{B}^{ext} \left( \sum_{i=1}^{N_c} q_i \right) + \boldsymbol{\omega} \times \left( \sum_{i=1}^{N_c} q_i \mathbf{r}_{cm \rightarrow i} \right) \times \mathbf{B}^{ext}, \end{aligned} \quad (2.23)$$

and, similarly, for the total external moment about the center of mass,

$$\begin{aligned} \mathbf{M}_{cm}^{EXT} &= \sum_{i=1}^{N_c} \mathbf{r}_{cm \rightarrow i} \times \left( \underbrace{q_i \mathbf{E}^{ext}}_{\text{electrical contribution}} + \underbrace{q_i (\mathbf{v}_{cm} \times \mathbf{B}^{ext})}_{\text{linear velocity contribution}} \right. \\ &\quad \left. + \underbrace{q_i ((\boldsymbol{\omega} \times \mathbf{r}_{cm \rightarrow i}) \times \mathbf{B}^{ext})}_{\text{angular velocity contribution}} \right) \\ &= \left( \sum_{i=1}^{N_c} q_i \mathbf{r}_{cm \rightarrow i} \right) \times \mathbf{E}^{ext} + \left( \sum_{i=1}^{N_c} q_i \mathbf{r}_{cm \rightarrow i} \right) \times \mathbf{v}_{cm} \times \mathbf{B}^{ext} \\ &\quad + \left( \sum_{i=1}^{N_c} q_i \mathbf{r}_{cm \rightarrow i} \times \boldsymbol{\omega} \times \mathbf{r}_{cm \rightarrow i} \right) \times \mathbf{B}^{ext} \\ &= \mathbf{R}_q \times \mathbf{E}^{ext} + \mathbf{R}_q \times \mathbf{v}_{cm} \times \mathbf{B}^{ext} + \mathbf{H}_q \times \mathbf{B}^{ext}, \end{aligned} \quad (2.24)$$

where

- $\mathbf{R}_q \stackrel{\text{def}}{=} \sum_{i=1}^{N_c} q_i \mathbf{r}_{cm \rightarrow i}$  is defined as the *center of charge relative to the center of mass* and
- $\mathbf{H}_q \stackrel{\text{def}}{=} \sum_{i=1}^{N_c} q_i \frac{\mathbf{H}_{cm \rightarrow i}}{m_i}$  is defined as the *charged angular momentum per unit mass with respect to the center of mass*.

Thus, the following three quantities play a central role in the cluster behavior:

- The sum of the individual charges (“overall charge”/first moment):  $Q \stackrel{\text{def}}{=} \sum_{i=1}^{N_c} q_i$ ,
- The sum of the distances between the individual charged particles ( $\mathbf{r}_i$ ) and the center of mass of the cluster ( $\mathbf{r}_{cm}$ ), weighted by the individual charges (“charged radius”/second-moment):  $\mathbf{R}_q \stackrel{\text{def}}{=} \sum_{i=1}^{N_c} q_i (\mathbf{r}_i - \mathbf{r}_{cm})$ ,
- The sum of the self-cross-product of the distances between the individual charged particles and the center of mass of the cluster, weighted by the individual charges ( $\bar{\mathcal{I}}_q$ , “moment of charge”/third-moment):  $\mathbf{H}_q = \bar{\mathcal{I}}_q \cdot \boldsymbol{\omega} \stackrel{\text{def}}{=} \sum_{i=1}^{N_c} q_i (\mathbf{r}_i - \mathbf{r}_{cm}) \times$

$\boldsymbol{\omega} \times (\mathbf{r}_i - \mathbf{r}_{cm})$ , where  $\boldsymbol{\omega}$  is the angular velocity of the body and where  $\bar{\mathcal{I}}_q$  has components  $(p, s = 1, 2, 3)$

$$\bar{\mathcal{I}}_{q,ps} = \sum_{i=1}^{N_c} q_i (||\mathbf{r}_i - \mathbf{r}_{cm}||^2 \delta_{ps} - \hat{x}_{ip} \hat{x}_{is}). \quad (2.25)$$

### 2.2.2 Various Charge Distribution Cases

In summary, for a charged cluster, the governing equations may be written as

$$\mathcal{M}\ddot{\mathbf{r}}_{cm} = \mathcal{M}\dot{\mathbf{v}}_{cm} = \boldsymbol{\Psi}^{EXT} = \underbrace{QE^{ext}}_{\mathcal{T}_1} + \underbrace{Q\mathbf{v}_{cm} \times \mathbf{B}^{ext}}_{\mathcal{T}_2} + \underbrace{(\boldsymbol{\omega} \times \mathbf{R}_q) \times \mathbf{B}^{ext}}_{\mathcal{T}_3}, \quad (2.26)$$

and

$$\dot{\mathbf{H}}_{cm} = \frac{d(\bar{\mathcal{I}} \cdot \boldsymbol{\omega})}{dt} = \mathbf{M}_{cm}^{EXT} = \underbrace{\mathbf{R}_q \times \mathbf{E}^{ext}}_{\mathcal{T}_4} + \underbrace{\mathbf{R}_q \times \mathbf{v}_{cm} \times \mathbf{B}^{ext}}_{\mathcal{T}_5} + \underbrace{(\bar{\mathcal{I}}_q \cdot \boldsymbol{\omega}) \times \mathbf{B}^{ext}}_{\mathcal{T}_6}. \quad (2.27)$$

One may observe that:

- In the special case when the overall charge ( $Q$ ) of the cluster is zero (neutral),  $\mathcal{T}_1 = \mathcal{T}_2 = 0$ ,
- In the special case when the overall charged distances are evenly distributed with respect to the mass center,  $\mathbf{R}_q = \mathbf{0} \Rightarrow \mathcal{T}_3 = \mathcal{T}_4 = \mathcal{T}_5 = \mathbf{0}$ ,
- In the special case when the overall charged moment ( $\bar{\mathcal{I}}_q$ ) is zero,  $\mathcal{T}_6 = 0$ .

Also, one has

$$\begin{aligned} ||\boldsymbol{\Psi}^{EXT}|| &= ||Q(\mathbf{E}^{ext} + \mathbf{v}_{cm} \times \mathbf{B}^{ext}) + (\boldsymbol{\omega} \times \mathbf{R}_q) \times \mathbf{B}^{ext}|| \\ &\leq |Q| ||\mathbf{E}^{ext} + \mathbf{v}_{cm} \times \mathbf{B}^{ext}|| + ||\mathbf{R}_q|| ||\boldsymbol{\omega}|| ||\mathbf{B}^{ext}|| \\ &\leq |Q| ||\mathbf{E}^{ext}|| + |Q| ||\mathbf{v}_{cm}|| ||\mathbf{B}^{ext}|| + ||\mathbf{R}_q|| ||\boldsymbol{\omega}|| ||\mathbf{B}^{ext}|| \end{aligned} \quad (2.28)$$

and

$$\begin{aligned} ||\mathbf{M}_{cm}^{EXT}|| &= ||\mathbf{R}_q \times (\mathbf{E}^{ext} + \mathbf{v}_{cm} \times \mathbf{B}^{ext}) + (\bar{\mathcal{I}}_q \cdot \boldsymbol{\omega}) \times \mathbf{B}^{ext}|| \\ &\leq ||\mathbf{R}_q|| ||\mathbf{E}^{ext} + \mathbf{v}_{cm} \times \mathbf{B}^{ext}|| + ||\bar{\mathcal{I}}_q|| ||\boldsymbol{\omega}|| ||\mathbf{B}^{ext}|| \\ &\leq ||\mathbf{R}_q|| ||\mathbf{E}^{ext}|| + ||\mathbf{R}_q|| ||\mathbf{v}_{cm}|| ||\mathbf{B}^{ext}|| + ||\bar{\mathcal{I}}_q|| ||\boldsymbol{\omega}|| ||\mathbf{B}^{ext}||. \end{aligned} \quad (2.29)$$

Thus, both  $Q$  and  $||\mathbf{R}_q||$  must be zero for  $||\boldsymbol{\Psi}^{EXT}|| = 0$ , while both  $||\mathbf{R}_q||$  and  $||\bar{\mathcal{I}}_q||$  must be zero for  $||\mathbf{M}_{cm}^{EXT}|| = 0$ . Clearly, each of the (zero/nonzero) cases can occur independently of one another.

*Remark* The dynamics of a general cluster must be treated numerically, particularly when one has a three-dimensional body with a complex charge distribution. This is discussed next.

## 2.3 Numerical Methods for the Dynamics of a Charged Cluster

We now treat the dynamics of a cluster numerically. We first focus on the translational motion of the center of mass, and then turn to the rotational contribution.

### 2.3.1 Cluster Translational Contribution

The translational component of the center of mass can be written as

$$\mathcal{M}\ddot{\mathbf{r}}_{cm} = \mathcal{M}\dot{\mathbf{v}}_{cm} = \boldsymbol{\Psi}^{EXT}. \quad (2.30)$$

A trapezoidal time-stepping rule is used, whereby at some intermediate moment in time  $t \leq t + \phi\Delta t \leq t + \Delta t$  ( $0 \leq \phi \leq 1$ ),

$$\dot{\mathbf{v}}_{cm}(t + \phi\Delta t) \approx \frac{\mathbf{v}_{cm}(t + \Delta t) - \mathbf{v}_{cm}(t)}{\Delta t} \quad (2.31)$$

$$= \frac{1}{\mathcal{M}} \boldsymbol{\Psi}^{EXT}(t + \phi\Delta t) \quad (2.32)$$

$$\approx \frac{1}{\mathcal{M}} \left( \phi \boldsymbol{\Psi}^{EXT}(t + \Delta t) + (1 - \phi) \boldsymbol{\Psi}^{EXT}(t) \right), \quad (2.33)$$

leading to

$$\mathbf{v}_{cm}(t + \Delta t) = \mathbf{v}_{cm}(t) + \frac{\Delta t}{\mathcal{M}} \left( \phi \boldsymbol{\Psi}^{EXT}(t + \Delta t) + (1 - \phi) \boldsymbol{\Psi}^{EXT}(t) \right). \quad (2.34)$$

For the position, we have

$$\begin{aligned} \dot{\mathbf{r}}_{cm}(t + \phi\Delta t) &\approx \frac{\mathbf{r}_{cm}(t + \Delta t) - \mathbf{r}_{cm}(t)}{\Delta t} \approx \mathbf{v}_{cm}(t + \phi\Delta t) \\ &\approx (\phi \mathbf{v}_{cm}(t + \Delta t) + (1 - \phi) \mathbf{v}_{cm}(t)), \end{aligned} \quad (2.35)$$



leading to

$$\mathbf{r}_{cm}(t + \Delta t) = \mathbf{r}_{cm}(t) + \Delta t (\phi \mathbf{v}_{cm}(t + \Delta t) + (1 - \phi) \mathbf{v}_{cm}(t)). \quad (2.36)$$

### 2.3.2 Cluster Rotational Motion

There are two possible approaches to compute the cluster rotations, either using an (1) inertially-fixed frame or (2) a body-fixed frame. We employ an inertially-fixed approach, and implicit time-stepping for the duration of this chapter. This straightforward approach entails, at each (implicit) time step, decomposing an increment of motion into an incremental rigid body translational contribution and an incremental rigid body rotational contribution (rotation about the center of mass). The rotational contribution is determined by solving a set of coupled nonlinear equations governing the angular velocity and the incremental rotation of the body around the axis of rotation (which also changes as a function of time). The equation for the angular momentum can be written as

$$\dot{\mathbf{H}}_{cm} = \frac{d(\bar{\mathcal{I}} \cdot \boldsymbol{\omega})}{dt} = \mathbf{M}_{cm}^{EXT}. \quad (2.37)$$

Because the body rotates,  $\bar{\mathcal{I}}$  is implicitly dependent on  $\boldsymbol{\omega}$  (and hence time), which leads to a coupled system of nonlinear ODE's which can be solved with an iterative scheme. Equation 2.37 is discretized by a trapezoidal scheme (as for the translational component)

$$\frac{d(\bar{\mathcal{I}} \cdot \boldsymbol{\omega})}{dt} \Big|_{t+\phi\Delta t} = \frac{(\bar{\mathcal{I}} \cdot \boldsymbol{\omega})|_{t+\Delta t} - (\bar{\mathcal{I}} \cdot \boldsymbol{\omega})|_t}{\Delta t}, \quad (2.38)$$

thus leading to

$$(\bar{\mathcal{I}} \cdot \boldsymbol{\omega})|_{t+\Delta t} = (\bar{\mathcal{I}} \cdot \boldsymbol{\omega})|_t + \Delta t \mathbf{M}_{cm}^{EXT}(t + \phi\Delta t). \quad (2.39)$$

Solving for  $\boldsymbol{\omega}(t + \Delta t)$  yields

$$\boldsymbol{\omega}(t + \Delta t) = \left( \bar{\mathcal{I}}(t + \Delta t) \right)^{-1} \cdot \left( (\bar{\mathcal{I}} \cdot \boldsymbol{\omega})|_t + \Delta t \mathbf{M}_{cm}^{EXT}(t + \phi\Delta t) \right), \quad (2.40)$$

where

$$\mathbf{M}_{cm}^{EXT}(t + \phi\Delta t) \approx \phi \mathbf{M}_{cm}^{EXT}(t + \Delta t) + (1 - \phi) \mathbf{M}_{cm}^{EXT}(t), \quad (2.41)$$

which yields an implicit nonlinear equation, of the form  $\boldsymbol{\omega}(t + \Delta t) = \mathcal{F}(\boldsymbol{\omega}(t + \Delta t))$  since the moment of inertia is a function of time,  $\bar{\mathcal{I}}(t + \Delta t)$ , due to the body's rotation. An iterative, implicit, solution scheme may be written as (for iterations  $K = 1, 2, \dots$ )

$$\boldsymbol{\omega}^{K+1}(t + \Delta t) = \left( \bar{\mathcal{I}}^K(t + \Delta t) \right)^{-1} \cdot \left( (\bar{\mathcal{I}} \cdot \boldsymbol{\omega})|_t + \Delta t \mathbf{M}_{cm}^{EXT,K}(t + \phi \Delta t) \right), \quad (2.42)$$

where  $\bar{\mathcal{I}}^K(t + \Delta t)$  can be computed by a similarity transform (described shortly).<sup>3</sup> After the update for  $\boldsymbol{\omega}^{K+1}(t + \Delta t)$  has been computed (utilizing the  $\bar{\mathcal{I}}^K(t + \Delta t)$  from the previous iteration), the rotation of the body about the center of mass can be determined. The *incremental* angular rotation around the instantaneous rotation axis  $\mathbf{a}^{K+1}(t + \phi \Delta t)$  (which will also have to be updated) is obtained by  $(\boldsymbol{\omega}^{K+1}(t + \phi \Delta t) = \omega^{K+1}(t + \phi \Delta t) \mathbf{a}^{K+1}(t + \phi \Delta t))$

$$\frac{d\theta^{K+1}}{dt}(t + \phi \Delta t) = \omega^{K+1}(t + \phi \Delta t) \approx \frac{\Delta \theta^{K+1}(t + \phi \Delta t)}{\Delta t}, \quad (2.43)$$

where  $\omega^{K+1}(t + \phi \Delta t) = \|\boldsymbol{\omega}^{K+1}(t + \phi \Delta t)\|$  being a *scalar* rotation rate about the instantaneous axis ( $\Delta \theta^{K+1}(t + \phi \Delta t)$  is the corresponding incremental rotation about that instantaneous axis),

$$\mathbf{a}^{K+1}(t + \phi \Delta t) \stackrel{\text{def}}{=} \frac{\boldsymbol{\omega}^{K+1}(t + \phi \Delta t)}{\|\boldsymbol{\omega}^{K+1}(t + \phi \Delta t)\|} \approx \frac{\phi \boldsymbol{\omega}^{K+1}(t + \Delta t) + (1 - \phi) \boldsymbol{\omega}(t)}{\|\phi \boldsymbol{\omega}^{K+1}(t + \Delta t) + (1 - \phi) \boldsymbol{\omega}(t)\|}, \quad (2.44)$$

and thus

$$\Delta \theta^{K+1}(t + \phi \Delta t) = \omega^{K+1}(t + \phi \Delta t) \Delta t, \quad (2.45)$$

where  $\omega^{K+1}(t + \phi \Delta t) = \|\phi \boldsymbol{\omega}^{K+1}(t + \Delta t) + (1 - \phi) \boldsymbol{\omega}(t)\|$ . To determine the movement of the individual points/particles in the rigid (cluster) body, we need to perform a rigid body translation and rotation (described in the next section). For example, consider a point  $\mathbf{r}_i$  on the body. The update would be

$$\mathbf{r}_i(t + \Delta t) = \mathbf{r}_i(t) + \underbrace{\mathbf{u}_{cm}}_{\text{due to cm translation}} + \underbrace{\mathbf{u}_{i,rot}}_{\text{due to rotation wrt cm}} \quad (2.46)$$

where

$$\mathbf{u}_{cm} = \mathbf{r}_{cm}(t + \Delta t) - \mathbf{r}_{cm}(t), \quad (2.47)$$

and where  $\mathbf{u}_{i,rot}$  is a contribution due to an incremental rotation of the relative position vector

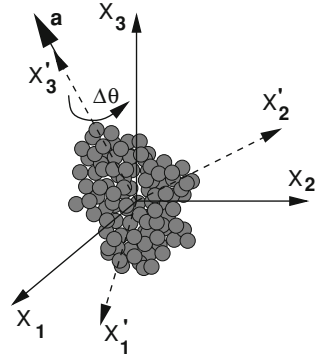
$$\boldsymbol{\tau}^{(i)} \stackrel{\text{def}}{=} \mathbf{r}_i(t) - \mathbf{r}_{cm}(t) \quad (2.48)$$

by  $\Delta \theta$  about the center of mass (Fig. 2.3).

---

<sup>3</sup> One may view the overall process as a fixed-point calculation of the form  $\boldsymbol{\omega}^{K+1}(t + \Delta t) = \mathcal{F}(\boldsymbol{\omega}^K(t + \Delta t))$ .

**Fig. 2.3** Aligning the primed coordinate system with the instantaneous axis of rotation ( $\mathbf{a}$ ) for a cluster (Zohdi [44])



### 2.3.3 Transformation Matrices for Updates and Incremental Rotation

In order to rotate any point  $i$ , with position vector  $\boldsymbol{\tau}^{(i)}$ , associated with the rigid body, we require some standard transformations. The same transformation is needed to rotate the body's moment of inertia,  $\bar{\mathcal{I}}$  (Fig. 2.3). It is a relatively standard exercise in linear algebra to show that any vector,  $\boldsymbol{\tau}$ , which can be expressed in either the unprimed or primed basis,  $\boldsymbol{\tau} = (\boldsymbol{\tau} \cdot \mathbf{e}_i)\mathbf{e}_i = (\boldsymbol{\tau} \cdot \mathbf{e}'_j)\mathbf{e}'_j$ , where summation index notation is employed. These two representations are explicitly related by

$$\begin{bmatrix} \tau_1 \\ \tau_2 \\ \tau_3 \end{bmatrix}' = \underbrace{\begin{bmatrix} \mathbf{e}_1 \cdot \mathbf{e}'_1 & \mathbf{e}_2 \cdot \mathbf{e}'_1 & \mathbf{e}_3 \cdot \mathbf{e}'_1 \\ \mathbf{e}_1 \cdot \mathbf{e}'_2 & \mathbf{e}_2 \cdot \mathbf{e}'_2 & \mathbf{e}_3 \cdot \mathbf{e}'_2 \\ \mathbf{e}_1 \cdot \mathbf{e}'_3 & \mathbf{e}_2 \cdot \mathbf{e}'_3 & \mathbf{e}_3 \cdot \mathbf{e}'_3 \end{bmatrix}}_{[A]} \begin{bmatrix} \tau_1 \\ \tau_2 \\ \tau_3 \end{bmatrix}. \quad (2.49)$$

Note that  $\mathbf{A}^{-1} = \mathbf{A}^T$ , and thus  $\boldsymbol{\tau}' = \mathbf{A} \cdot \boldsymbol{\tau}$  and  $\boldsymbol{\tau} = \mathbf{A}^T \cdot \boldsymbol{\tau}'$ . This basic result can be used to perform rotation of a vector about an axis, as well as the rotation of the inertia tensor. Without any loss of generality, we align the  $\mathbf{e}'_3$  axis to instantaneous rotation axis  $\mathbf{a}$ . The total transformation (rotation) of a vector  $\boldsymbol{\tau}^{(i)}$  representing a point  $i$  on the body can be represented by

$$\begin{aligned} [\boldsymbol{\tau}^{(i)}]^{rot} &= [\mathbf{A}]^T [\mathbf{R}(\Delta\theta)] \underbrace{[\mathbf{A}][\boldsymbol{\tau}_i]}_{[\boldsymbol{\tau}^{(i)}]'} \\ &\quad \underbrace{[\boldsymbol{\tau}^{(i)}]^{rot, t}}_{[\boldsymbol{\tau}^{(i)}]^{rot}} \end{aligned} \quad (2.50)$$

where

$$[\mathbf{R}(\Delta\theta)] = \begin{bmatrix} \cos(\Delta\theta) & -\sin(\Delta\theta) & 0 \\ \sin(\Delta\theta) & \cos(\Delta\theta) & 0 \\ 0 & 0 & 1 \end{bmatrix}. \quad (2.51)$$

Similarly, for the rotation inertia tensor,

$$[\bar{\mathcal{I}}]^{rot} = [\mathbf{A}]^T [\mathbf{R}(\Delta\theta)] \underbrace{[\mathbf{A}][\bar{\mathcal{I}}][\mathbf{A}]^T}_{[\bar{\mathcal{I}}']} [\mathbf{R}(\Delta\theta)]^T [\mathbf{A}], \quad (2.52)$$

$$\underbrace{\hspace{10em}}_{[\bar{\mathcal{I}}]^{rot, '}} \underbrace{\hspace{10em}}_{[\bar{\mathcal{I}}]^{rot}}$$

where, during the iterative calculations,  $[\bar{\mathcal{I}}] = [\bar{\mathcal{I}}(t)]$  and  $[\bar{\mathcal{I}}]^{rot} = [\bar{\mathcal{I}}(t + \Delta t)]$ .

### 2.3.4 Algorithmic Procedure

The overall procedure is as follows, at time  $t$ :

1. Compute the new position of the center of mass.
2. Compute (iteratively) the incremental angular rotation of the body with respect to the center of mass until system convergence:

$$||\boldsymbol{\omega}^{K+1}(t + \Delta t) - \boldsymbol{\omega}^K(t + \Delta t)|| \leq TOL ||\boldsymbol{\omega}^{K+1}(t + \Delta t)||. \quad (2.53)$$

This requires a rotation of the body within the iterations:

- (a) Update  $\boldsymbol{\omega}^{K+1}(t + \Delta t)$  (assuming that  $\boldsymbol{\omega}^K(t + \Delta t)$  has been computed)

$$\boldsymbol{\omega}^{K+1}(t + \Delta t) = \left( \bar{\mathcal{I}}^K(t + \Delta t) \right)^{-1} \cdot \left( (\bar{\mathcal{I}} \cdot \boldsymbol{\omega})|_t + \Delta t \mathbf{M}_{cm}^{EXT, K}(t + \phi \Delta t) \right). \quad (2.54)$$

- (b) Compute the (updated) axis of rotation:

$$\mathbf{a}^{K+1}(t + \phi \Delta t) \stackrel{\text{def}}{=} \frac{\boldsymbol{\omega}^{K+1}(t + \phi \Delta t)}{||\boldsymbol{\omega}^{K+1}(t + \phi \Delta t)||} \approx \frac{\phi \boldsymbol{\omega}^{K+1}(t + \Delta t) + (1 - \phi) \boldsymbol{\omega}(t)}{||\phi \boldsymbol{\omega}^{K+1}(t + \Delta t) + (1 - \phi) \boldsymbol{\omega}(t)||}. \quad (2.55)$$

- (c) Compute the basis  $\mathbf{e}'_3$ -aligned instantaneous axis of rotation ( $\mathbf{a}$ ):

- (i)  $\mathbf{e}'_3$ , is aligned with  $\mathbf{a}^{K+1}$
- (ii)  $\mathbf{e}'_1 = \mathbf{e}'_3 \times \mathbf{e}_3 / ||\mathbf{e}'_3 \times \mathbf{e}_3||$  and
- (iii)  $\mathbf{e}'_2 = \mathbf{e}'_3 \times \mathbf{e}'_1 / ||\mathbf{e}'_3 \times \mathbf{e}'_1||$ .

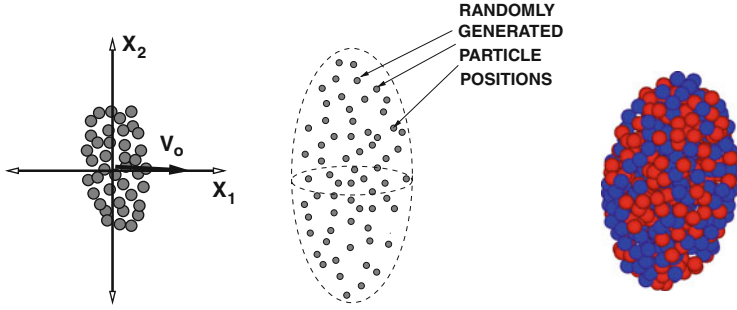


**Fig. 2.4** *Left* the initial configuration. *Middle* an ellipsoidal envelope for the random particle positions. *Right* the actual object used in computations (*blue* is a base-positive charge and *red* is a base-negative charge) (Zohdi [44])

- (d) Compute incremental angle of rotation  $\Delta\theta^{K+1}(t + \phi\Delta t)$  and the composite transformation for the inertia tensor in Eq. 2.52 and obtain the update  $\bar{\mathcal{I}}^{K+1}(t + \Delta t)$ .
  - (e) Compute the total new position of the points in the body ( $i$ ) with Eqs. 2.50 and 2.46.
  - (f) Repeat steps (a)–(e) until Eq. 2.53 is satisfied.
3. Increment time forward and repeat the procedure.

## 2.4 Model Problems/Numerical Examples

As a model problem, we consider a cluster formed by randomly dispersing charged particulates within a prolate ellipsoidal domain (aspect ratio of 2:1, Fig. 2.4). The radii of the ellipsoidal domain (envelope) in which the particles were randomly dispersed were 0.002 m (major axis) and 0.001 m (for both minor axes).<sup>4</sup> We considered  $N_c = 500$  randomly distributed particles, with an overall charge of the body set to  $\sum_{i=1}^{N_c} q_i = q^* = 0.01$  Coulomb, where for  $q_i = \pm q_o + q^*/N_c$ . There were 250 base-positive ( $q_o = +0.001$ ) and 250 base-negative ( $q_o = -0.001$ ) particles in the system. The radii of the individual particles were set to  $r = 0.0001$  m.<sup>5</sup>

In order to help investigate what type of motion a charged cluster will experience, we consider a “comparison” case when only a single charged particle (or, considered equivalently, a lumped charged mass) is present in the system, with position vector

<sup>4</sup> The absolute length-scales, charges and masses are somewhat irrelevant to the model problem framework, and can be scaled to any desired value for specific application.

<sup>5</sup> The densities for the particles were uniformly assigned  $\rho = 2000$  kg/m<sup>3</sup>, with masses given by  $m = \rho \frac{4}{3} \pi R^3$  kg.

denoted by  $\mathbf{r}_s$ , governed by Eq. 2.1, written in a slightly different form as ( $\dot{\mathbf{r}}_s = \mathbf{v}_s$ )<sup>6</sup>

$$m_s \ddot{\mathbf{r}}_s = q_s (\mathbf{E}^{ext} + \dot{\mathbf{r}}_s \times \mathbf{B}^{ext}). \quad (2.56)$$

The difference in the solution path for the single particle (governed by Eq. 2.56) and a multiparticle cluster, with center of mass given by  $\mathbf{r}_{cm}$  (governed by Eq. 2.26 and implicitly by 2.27), can be characterized by taking the difference between Eqs. 2.26 and 2.56 to obtain

$$\mathcal{M} \ddot{\mathbf{r}}_{cm} - m \ddot{\mathbf{r}}_s = (Q - q_s) \mathbf{E}^{ext} + (Q \dot{\mathbf{r}}_{cm} - q_s \dot{\mathbf{r}}_s) \times \mathbf{B}^{ext} + (\boldsymbol{\omega} \times \mathbf{R}_q \times \mathbf{B}^{ext}). \quad (2.57)$$

If we assume  $Q = q_s$ ,  $M = m_s$  and define  $\mathcal{E} \stackrel{\text{def}}{=} \mathbf{r}_{cm} - \mathbf{r}_s$ , we obtain a “deviation” equation governing the difference in the trajectories of the two systems, that is,

$$\ddot{\mathcal{E}} = \frac{1}{\mathcal{M}} (Q \dot{\mathcal{E}} \times \mathbf{B}^{ext} + \boldsymbol{\omega} \times \mathbf{R}_q \times \mathbf{B}^{ext}). \quad (2.58)$$

In the special case when  $\mathbf{B}^{ext} = \mathbf{0}$ , the difference between the motion of the center of mass is zero ( $\mathcal{E}(t) = 0$ ), although one can still expect rotation about the center of mass for the cluster, via  $\boldsymbol{\omega}$ , which is dictated by Eq. 2.27.

### 2.4.1 Special Case # 1: No Magnetic Field ( $\mathbf{E}^{ext} \neq \mathbf{0}$ and $\mathbf{B}^{ext} = \mathbf{0}$ )

In the special case when there is no magnetic field, if  $\mathbf{r}_s(t=0) = \mathbf{0}$ ,  $\mathbf{v}_s(t=0) = v_o \mathbf{e}_1$ ,  $\mathbf{B}^{ext} = \mathbf{0}$  and  $\mathbf{E}^{ext} = E^{ext} \mathbf{e}_3$ , the solution for the dynamics of a single particle is

$$\begin{Bmatrix} v_{s1}(t) \\ v_{s2}(t) \\ v_{s3}(t) \end{Bmatrix} = \begin{Bmatrix} v_o \\ 0 \\ \frac{q_s}{m_s} E_3^{ext} t \end{Bmatrix} \Rightarrow \begin{Bmatrix} r_{s1}(t) \\ r_{s2}(t) \\ r_{s3}(t) \end{Bmatrix} = \begin{Bmatrix} v_o t \\ 0 \\ \frac{q_s}{2m_s} E_3^{ext} t^2 \end{Bmatrix}. \quad (2.59)$$

Now, for a cluster,<sup>7</sup> let us (numerically) consider this special case ( $\mathbf{v}(t=0) = 0.01 \mathbf{e}_1$ ,  $\boldsymbol{\omega}(t=0) = \mathbf{0}$ ,  $\mathbf{B}^{ext} = \mathbf{0}$  and  $\mathbf{E}^{ext} = 0.1 \mathbf{e}_3$ ), which should yield results similar to a single particle in Eq. 2.59. Indeed, as shown in Fig. 2.5, as in the single particle case, when  $\mathbf{B}^{ext} = \mathbf{0}$ , we have the predicted motion, i.e., the center of mass

<sup>6</sup> Note: The governing Eq. 2.56, written in component form is, for component 1:  $\dot{v}_{s1} = \frac{q_s}{m_s} (E_1^{ext} + (v_{s2} B_3^{ext} - v_{s3} B_2^{ext}))$ , for component 2:  $\dot{v}_{s2} = \frac{q_s}{m_s} (E_2^{ext} - (v_{s1} B_3^{ext} - v_{s3} B_1^{ext}))$ , and for component 3:  $\dot{v}_{s3} = \frac{q_s}{m_s} (E_3^{ext} + (v_{s1} B_2^{ext} - v_{s2} B_1^{ext}))$ . These equations can be solved analytically. There are a variety of possible particle trajectories, and we refer the reader to Jackson [13].

<sup>7</sup> These specific parameter choices resulted in  $\|\mathbf{R}_q\| = 0.00297$  and  $\|\mathbf{\bar{T}}_q\| = 0.0000229$ . The simulations were run for other large clusters with similar trends occurring. In other words, these results are representative. The overall approach is general, and is valid for any distribution of charges.

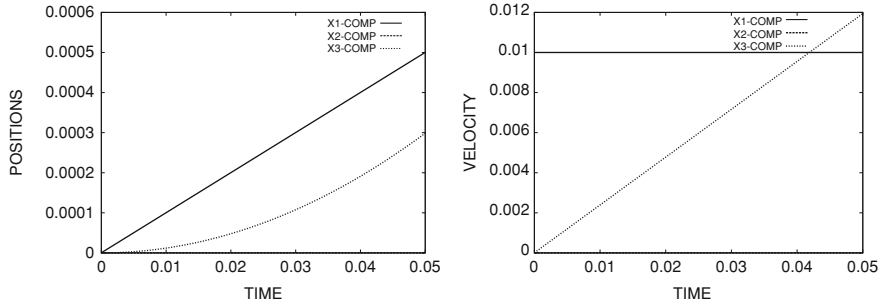
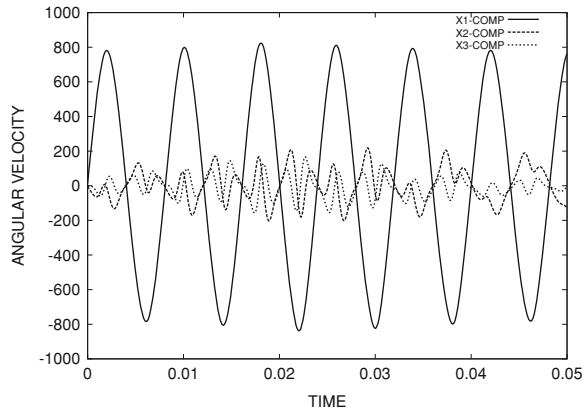


**Fig. 2.5** Special case 1:  $\mathbf{v}(t=0) = 0.01\mathbf{e}_1$ ,  $\mathbf{B}^{ext} = \mathbf{0}$  and  $\mathbf{E}^{ext} = 0.1\mathbf{e}_3$ . *Left* the position of the center of mass. *Right* the velocity of the center of mass. The trajectory of the center of mass of the cluster is similar to that of a single charged particle (Zohdi [44])

**Fig. 2.6** Special case 1:  $\mathbf{v}(t=0) = 0.01\mathbf{e}_1$ ,  $\mathbf{B}^{ext} = \mathbf{0}$  and  $\mathbf{E}^{ext} = 0.1\mathbf{e}_3$ : the angular velocity. The rotation about the center of mass is induced entirely by the electric field (Zohdi [44])



of a cluster behaves similarly to that of a single particle. Notice in Fig. 2.6, because of the term  $\mathcal{T}_4 \neq 0$  in Eq. 2.27, however, that there is rotational motion about the center of mass. This rotation (a twisting back and forth) about the center of mass is purely induced by the electric field. We emphasize, for this special case, because the only “forcing term” on the right hand side of the angular momentum Eq. 2.27 is  $\mathcal{T}_4 \stackrel{\text{def}}{=} \mathbf{R}_q \times \mathbf{E}^{ext}$  (since  $\mathbf{B}^{ext} = \mathbf{0}$ ),  $\mathbf{E}^{ext}$  is solely responsible for any spin of the cluster about its mass center. This term manifests the oscillations seen in Fig. 2.6 and is a phenomenon that is nonexistent in the single particle solution Eq. 2.59.

#### 2.4.2 Special Case # 2: No Electric Field ( $\mathbf{E}^{ext} = \mathbf{0}$ and $\mathbf{B}^{ext} \neq \mathbf{0}$ )

Now, consider a case with no electric field and a magnetic field present,  $\mathbf{r}_s(t=0) = \mathbf{0}$ ,  $\mathbf{v}_s(t=0) = v_o\mathbf{e}_1$ ,  $\mathbf{B}^{ext} = B_3^{ext}\mathbf{e}_3$  and  $\mathbf{E}^{ext} = \mathbf{0}$ . Consequently, for a single particle, the solution is

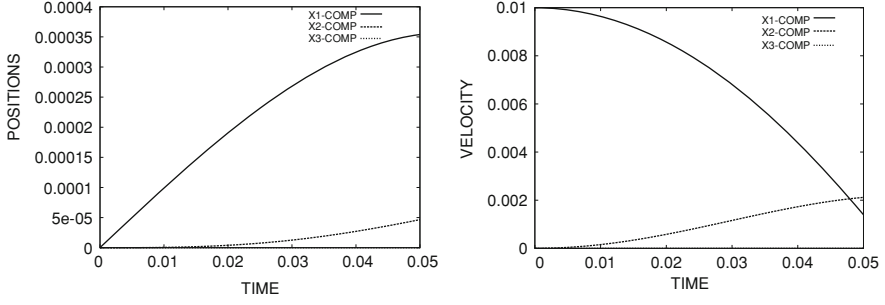


**Fig. 2.7** Special case 2:  $\mathbf{v}(t=0) = 0.01\mathbf{e}_1$ ,  $\mathbf{B}^{ext} = 0.01\mathbf{e}_3$  and  $\mathbf{E}^{ext} = \mathbf{0}$ . *Left* the position of the center of mass. *Right* the velocity of the center of mass (Zohdi [44])

$$\begin{Bmatrix} v_{s1}(t) \\ v_{s2}(t) \\ v_{s3}(t) \end{Bmatrix} = \begin{Bmatrix} v_o \cos \Omega_s t \\ -v_o \sin \Omega_s t \\ 0 \end{Bmatrix} \Rightarrow \begin{Bmatrix} r_{s1}(t) \\ r_{s2}(t) \\ r_{s3}(t) \end{Bmatrix} = \begin{Bmatrix} \frac{v_o}{\Omega_s} \sin \Omega_s t \\ \frac{v_o}{\Omega_s} (\cos \Omega_s t - 1) \\ 0 \end{Bmatrix}, \quad (2.60)$$

where  $\Omega_s = \frac{q_s B_3^{ext}}{m_s}$  is known as the cyclotron frequency. The cyclotron frequency (gyrofrequency) is the angular frequency at which a charged particle makes circular orbits in a plane perpendicular to the static magnetic field. Notice that when  $E_3^{ext} = 0$ , this traces out the equation of a circle centered at  $(0, \frac{-v_o}{\Omega_s}, 0)$ . The radius of the “magnetically-induced circle” (radius of oscillation) is<sup>8</sup>

$$\mathcal{R} \stackrel{\text{def}}{=} \frac{v_o}{\Omega_s} = \frac{v_o m_s}{q_s B_3^{ext}}. \quad (2.61)$$

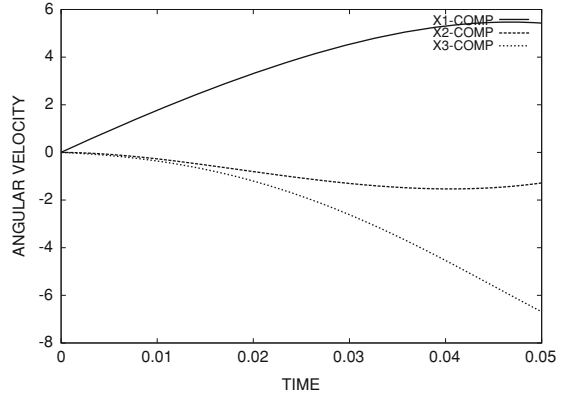
Thus, if a desired “turning radius” is denoted by  $\mathcal{R}$ , one may solve for the magnetic field that delivers the desired effect,  $B_3^{ext} = \frac{v_o m_s}{q_s \mathcal{R}}$ . We define the corresponding time period for one cycle to be completed as  $T \stackrel{\text{def}}{=} 2\pi / \Omega_s$ . For the parameters chosen, this results in  $\mathcal{R} = 0.0004188$  m,  $\Omega_s = 23.87$  rad/s and  $T = 0.1315$  s. For a cluster (numerically computed with an initial  $\omega(t=0)$ ), Fig. 2.7 illustrates motion with a possible long range period  $T$  and “large-scale” turning (cyclotron) radius ( $\mathcal{R}$ ) that is similar to that of a single particle.<sup>9</sup> Figure 2.8 indicates that there is some slight rotation of the body around the center of mass.

<sup>8</sup> As mentioned earlier, this field generates helical motion in three dimensions when  $\mathbf{E}^{ext} \neq \mathbf{0}$ .

<sup>9</sup> Figure 2.7 illustrates approximately one-quarter of a period (total period  $T \approx 20$  s) and a cyclotron radius of  $\mathcal{R} \approx 0.0004$  m.



**Fig. 2.8** Special case 2:  
 $\mathbf{v}(t=0) = 0.01\mathbf{e}_1$ ,  
 $\mathbf{B}^{ext} = 0.01\mathbf{e}_3$  and  $\mathbf{E}^{ext} = \mathbf{0}$ :  
 the angular velocity (Zohdi  
 [44])



### 2.4.3 General Case # 3: Combined Electric and Magnetic Fields $(\mathbf{E}^{ext} \neq \mathbf{0} \text{ and } \mathbf{B}^{ext} \neq \mathbf{0})$

Now, consider both the electric and magnetic fields to be present,  $\mathbf{r}_s(t=0) = \mathbf{0}$ ,  $\mathbf{v}_s(t=0) = v_o\mathbf{e}_1$ ,  $\mathbf{B}^{ext} = B_3^{ext}\mathbf{e}_3$  and  $\mathbf{E}^{ext} = E_3^{ext}\mathbf{e}_3$ , consequently, for a single particle

$$\begin{Bmatrix} v_{s1}(t) \\ v_{s2}(t) \\ v_{s3}(t) \end{Bmatrix} = \begin{Bmatrix} v_o \cos \Omega_s t \\ -v_o \sin \Omega_s t \\ \frac{q_s}{m_s} E_3^{ext} t \end{Bmatrix} \Rightarrow \begin{Bmatrix} r_{s1}(t) \\ r_{s2}(t) \\ r_{s3}(t) \end{Bmatrix} = \begin{Bmatrix} \frac{v_o}{\Omega_s} \sin \Omega_s t \\ \frac{v_o}{\Omega_s} (\cos \Omega_s t - 1) \\ \frac{q_s}{2m_s} E_3^{ext} t^2 \end{Bmatrix}. \quad (2.62)$$

Let us now consider these parameters for a cluster ( $\mathbf{r}(t=0) = \mathbf{0}$ ,  $\boldsymbol{\omega}(t=0) = \mathbf{0}$ ,  $\mathbf{v}(t=0) = 0.01\mathbf{e}_1$ ,  $\mathbf{B}^{ext} = 0.01\mathbf{e}_3$  and  $\mathbf{E}^{ext} = 0.1\mathbf{e}_3$ ). As shown in Fig. 2.9, there is large-scale reversal of the  $x_1$  component with a superposed oscillatory “wobble.” As in special case # 2, there would be large-scale turning of the cluster, albeit slowly-induced, due to a (nonmonotonic) reversal of the  $x_1$  velocity, which would eventually trace out a helix-like path in the  $x_1 - x_2$  plane moving upwards in the  $x_3$  direction. The rotations about the center of mass are highly variable due to the random positions of the charged particles within the cluster. Figures 2.9 and 2.10 indicates the dramatic difference (due to the absence of the electric field) between special case # 2 and general case # 3, which is predicted by Eq. 2.58. The key observation is that the effects of  $\mathbf{E}^{ext}$  and  $\mathbf{B}^{ext}$  are strongly coupled via Eqs. 2.26 and 2.27, as opposed to uncoupled (as exhibited by Eqs. 2.60 and 2.62). One reason for this strong coupling is due to the dependence of  $\boldsymbol{\omega}$  on  $\mathbf{E}^{ext}$ , as exhibited by Eq. 2.27. Even when  $Q = q_s = 0$ , the trajectory deviation is governed by

$$\ddot{\mathbf{E}} = \frac{1}{\mathcal{M}} (\boldsymbol{\omega} \times \mathbf{R}_q \times \mathbf{B}^{ext}), \quad (2.63)$$

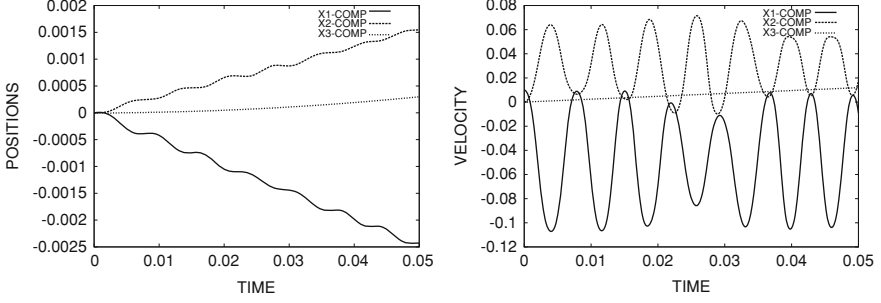


**Fig. 2.9** General case 3:  $\mathbf{v}(t=0) = 0.01\mathbf{e}_1$ ,  $\mathbf{B}^{ext} = 0.01\mathbf{e}_3$  and  $\mathbf{E}^{ext} = 0.1\mathbf{e}_3$ . *Left* the position of the center of mass. *Right* the velocity of the center of mass (Zohdi [44])

and is strongly influenced by a balance of angular momentum, through  $\boldsymbol{\omega}$ , which is governed by Eq. 2.27. The influence of  $\mathbf{E}^{ext}$  comes through Eq. 2.27, via term  $\mathcal{T}_4$ , even when  $Q = 0$ . We further note that in the special case when  $\mathbf{R}_q = \mathbf{0}$  and  $Q = q_s \neq 0$ , the deviation is governed by

$$\ddot{\mathbf{E}} = \frac{1}{\mathcal{M}} (Q \dot{\mathbf{E}} \times \mathbf{B}^{ext}), \quad (2.64)$$

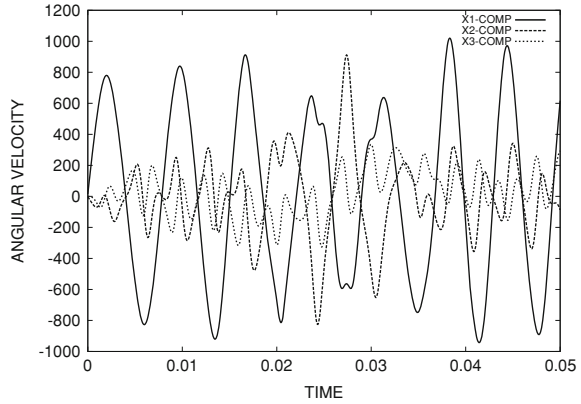
and the magnetic field plays a strong role in the deviation of the trajectories. One can still expect rotation about the center of mass for the cluster due to term  $\mathcal{T}_6$ , which is dependent on  $\bar{\mathcal{T}}_q$ , in Eq. 2.27, even when  $\mathbf{R}_q = \mathbf{0}$ .

## 2.5 Closing Remarks

It was shown that Eqs. 2.26 and 2.27 govern the dynamics of a charged cluster, and that the following three quantities play a central role in the cluster behavior:

- the sum of the individual ( $q_i$ ) charges:  $Q \stackrel{\text{def}}{=} \sum_{i=1}^{N_c} q_i$  (“overall charge” or the first moment),
- the sum of the distances between the individual charged particles ( $\mathbf{r}_i$ ) and the center of mass of the cluster ( $\mathbf{r}_{cm}$ ), weighted by the individual charges:  $\mathbf{R}_q \stackrel{\text{def}}{=} \sum_{i=1}^{N_p} q_i (\mathbf{r}_i - \mathbf{r}_{cm})$  (“charged radius” or the second-moment) and
- the sum of the self-cross-product of the distances between the individual charged particles and the center of mass of the cluster, weighted by the individual charges ( $\bar{\mathcal{T}}_q$ ):  $\mathbf{H}_q = \bar{\mathcal{T}}_q \cdot \boldsymbol{\omega} \stackrel{\text{def}}{=} \sum_{i=1}^{N_p} q_i (\mathbf{r}_i - \mathbf{r}_{cm}) \times \boldsymbol{\omega} \times (\mathbf{r}_i - \mathbf{r}_{cm})$ , where  $\boldsymbol{\omega}$  is the angular velocity of the body and  $\bar{\mathcal{T}}_q$  has components of  $(p, s = 1, 2, 3)$   $\bar{\mathcal{T}}_{q,ps} = \sum_{i=1}^{N_c} q_i (|\mathbf{r}_i - \mathbf{r}_{cm}|^2 \delta_{ps} - \hat{x}_{ip} \hat{x}_{is})$  (“moment of charge” or the third-moment).

**Fig. 2.10** General case 3:  
 $\mathbf{v}(t = 0) = 0.01\mathbf{e}_1$ ,  $\mathbf{B}^{ext} = 0.01\mathbf{e}_3$  and  $\mathbf{E}^{ext} = 0.1\mathbf{e}_3$ : the angular velocity (Zohdi [44])



In addition to dictating the motion of a cluster, these quantities control the differences in the motion of a charged cluster relative to that of a single charged particle. The deviation in dynamics of a charged cluster and a single charged particle (or lumped charged mass) is strongly influenced by the simultaneous presence of an electric and magnetic field. In particular, for large off-center charges, characterized by  $\mathbf{R}_q$  and  $\bar{\mathcal{I}}_q$ , the motion will vary significantly, and is governed by Eq. 2.58.

Independent of the purely scientific interest in the dynamics of a charged cluster, there are implications of these results for large-scale computation of particulate flows. Within the last decade, simultaneous advances in computational methods, applied mathematics and high-performance computing has raised the possibility that an analyst can directly numerically simulate (DNS) a process employing particulate flows containing several million particles, incorporating all of the important microscale details. A relatively straightforward DNS-type formulation of the dynamics of a multiparticulate system is to track the motion of  $i = 1, 2, \dots, N$  particles,

$$m_i \ddot{\mathbf{r}}_i = \Psi_i^{tot}(\mathbf{r}_1, \mathbf{r}_2, \dots, \mathbf{r}_{N_p}) = \Psi_i^{nf} + \Psi_i^{con} + q_i(\mathbf{E}^{ext} + \mathbf{v}_i \times \mathbf{B}^{ext}), \quad (2.65)$$

where  $\mathbf{r}_i$  is the position vector of the  $i$ th particle,  $\Psi_i^{tot}$  represents all forces acting on particle  $i$ ,  $\Psi_i^{nf}$  represents near-field inter-(charged)particle forces acting on particle  $i$ ,  $\Psi_i^{con}$  represents contact forces acting on particle  $i$  and where  $\mathbf{E}^{ext}$  and  $\mathbf{B}^{ext}$  are the external electromagnetic fields. The simulation of such flowing particulate systems has been extensively investigated for the last decade by Zohdi [27–45], employing numerical schemes based on high-performance iterative solvers, sorting-binning for fast interparticle calculations, Verlet lists, domain decomposition, parallel processing and temporally-adaptive methods. These types of formulations can easily describe the interaction of multiple particulate jets, jet breakup/disintegration and jet impact, where the application of continuum approaches is complex. The dynamics of clusters that evolve within a jet can be represented by directly describing the motion of each individual particle with the appropriate binding conditions (constraints) to its neighbors in the cluster, and is discussed next.

## References

1. Arbelaez, D., Zohdi, T. I., & Dornfeld, D. (2008). Modeling and simulation of material removal with particulate flow. *Computational Mechanics*, 42, 749–759.
2. Arbelaez, D., Zohdi, T. I., & Dornfeld, D. (2009). On impinging near-field granular jets. *International Journal for Numerical Methods in Fluids*.
3. Ciampini, D., Spelt, J. K., & Papini, M. (2003). Simulation of interference effects in particle streams following impact with a flat surface. Part I. Theory and analysis. *Wear*, 254, 237–249.
4. Ciampini, D., Spelt, J. K., & Papini, M. (2003). Simulation of interference effects in particle streams following impact with a flat surface. Part II. Parametric study and implications for erosion testing and blast cleaning. *Wear*, 254, 250–264.
5. Fish, J. (2006). Bridging the scales in nano engineering and science. *Journal of Nanoparticle Research*, 8, 577–594.
6. Frenklach, M., & Carmer, C. S. (1999). Molecular dynamics using combined quantum & empirical forces: Application to surface reactions. *Advances in Classical Trajectory Methods*, 4, 27–63.
7. Ghobeity, A., Krajac, T., Burzynski, T., Papini, M., & Spelt, J. K. (2008). Surface evolution models in abrasive jet micromachining. *Wear*, 264, 185–198.
8. Ghobeity, A., Spelt, J. K., & Papini, M. (2008). Abrasive jet micro-machining of planar areas and transitional slopes. *Journal of Micromechanics and Microengineering*, 18, 055014.
9. Ghosh, S., Valiveti, D. M., Harris, S. H., & Boileau, J. (2006). Microstructure characterization based domain partitioning as a pre-processor to multi-scale modeling of cast Aluminum alloys. *Modelling and Simulation in Material Science and Engineering*, 14, 1363–1396.
10. Gomes-Ferreira, C., Ciampini, D., & Papini, M. (2004). The effect of inter-particle collisions in erosive streams on the distribution of energy flux incident to a flat surface. *Tribology International*, 37, 791–807.
11. Haile, J. M. (1992). *Molecular dynamics simulations: Elementary methods*. New York: Wiley.
12. Hase, W. L. (1999). *Molecular dynamics of clusters, surfaces, liquids, and interfaces*. Advances in classical trajectory methods. (Vol. 4). Stamford: JAI Press.
13. Jackson, J. D. (1998). *Classical electrodynamics* (3rd ed.). New York: Wiley.
14. Luo, L., & Dornfeld, D. A. (2001). Material removal mechanism in chemical mechanical polishing: theory and modeling. *IEEE Transactions on Semiconductor Manufacturing*, 14(2), 112–133.
15. Luo, L., & Dornfeld, D. A. (2003). Material removal regions in chemical mechanical planarization for sub-micron integration for sub-micron integrated circuit fabrication: coupling effects of slurry chemicals, abrasive size distribution, and wafer-pad contact area. *IEEE Transactions on Semiconductor Manufacturing*, 16, 45–56.
16. Luo, L., & Dornfeld, D. A. (2003). Effects of abrasive size distribution in chemical-mechanical planarization: modeling and verification. *IEEE Transactions on Semiconductor Manufacturing*, 16, 469–476.
17. Luo, L., & Dornfeld, D. A. (2004). *Integrated modeling of chemical mechanical planarization of sub-micron IC fabrication*. New York: Springer.
18. Moelwyn-Hughes, E. A. (1961). *Physical Chemistry*. New York: Pergamon.
19. Rapaport, D. C. (1995). *The Art of Molecular Dynamics Simulation*. Cambridge: Cambridge University Press.
20. Rechtsman, M., Stillinger, F. H., & Torquato, S. (2005). Optimized interactions for targeted self-assembly: Application to honeycomb lattice. *Physical Review Letters*, 95, 228301.
21. Rechtsman, M., Stillinger, F. H., & Torquato, S. (2006). Designed interaction potentials via inverse methods for self-assembly. *Physical Review E*, 73, 011406.
22. Schlick, T. (2000). *Molecular modeling & simulation: An interdisciplinary guide*. New York: Springer.
23. Stillinger, F. H., & Weber, T. A. (1985). Computer simulation of local order in condensed phases of silicon. *Physical Review B*, 31, 5262–5271.

24. Tersoff, J. (1988). Empirical interatomic potential for carbon, with applications to amorphous carbon. *Physical Review Letters*, 61, 2879–2882.
25. Torquato, S. (2002). *Random heterogeneous materials: Microstructure and macroscopic properties*. New York: Springer.
26. Torquato, S. (2009). Inverse optimization techniques for targeted self-assembly. *Soft Matter*, 5, 1157.
27. Zohdi, T. I. (2002). An adaptive-recursive staggering strategy for simulating multifield coupled processes in microheterogeneous solids. *Internatioanl Journal for Numerical Methods in Engineering*, 53, 1511–1532.
28. Zohdi, T. I. (2003). Genetic design of solids possessing a random-particulate microstructure. *PTRS: Mathematical Physical and Engineering Sciences*, 361(1806), 1021–1043.
29. Zohdi, T. I. (2003). On the compaction of cohesive hyperelastic granules at finite strains. *Proceedings of the Royal Society*, 454(2034), 1395–1401.
30. Zohdi, T. I. (2003). Computational design of swarms. *Internatioanl Journal for Numerical Methods and Engineering*, 57, 2205–2219.
31. Zohdi, T. I. (2003). Constrained inverse formulations in random material design. *Computational Methods in Applied Mechanics and Engineering*, 1–20 192(28–30), 18, 3179–3194.
32. Zohdi, T. I. (2004). Modeling and simulation of a class of coupled thermo-chemo-mechanical processes in multiphase solids. *Computational Methods in, Applied Mechanics and Engineering*, 193(6–8), 679–699.
33. Zohdi, T. I. (2004). Modeling and direct simulation of near-field granular flows. *The International Journal of Solids Structures*, 42(2), 539–564.
34. Zohdi, T. I. (2004). A computational framework for agglomeration in thermo-chemically reacting granular flows. *Proceedings of the Royal Society*, 460(2052), 3421–3445.
35. Zohdi, T. I. (2005). Charge-induced clustering in multifield particulate flow. *International Journal of Numerical Methods and Engineering*, 62(7), 870–898.
36. Zohdi, T. I. (2006). Computation of the coupled thermo-optical scattering properties of random particulate systems. *Computational Methods in Applied Mechanics and Engineering*, 195, 5813–5830.
37. Zohdi, T. I. (2007). Computation of strongly coupled multifield interaction in particle-fluid systems. *Computational Methods in Applied Mechanics and Engrineering*, 196, 3927–3950.
38. Zohdi, T. I. (2007). Particle collision and adhesion under the influence of near-fields. *Journal of Mechanics of Materials and Structures*, 2(6), 1011–1018.
39. Zohdi, T. I. (2007). Introduction to the modeling and simulation of particulate flows. *Society for Industrial and Applied Mathematics*.
40. Zohdi, T. I. (2008). On the computation of the coupled thermo-electromagnetic response of continua with particulate microstructure. *International Journal of Numerical Methods in Engineering*, 76, 1250–1279.
41. Zohdi, T. I. (2009). Mechanistic modeling of swarms. *Computational Methods in Applied Mechanics and Engineering*, 198(21–26), 2039–2051.
42. Zohdi, T. I. (2010). Charged wall-growth in channel-flow. *International Journal of Engineering Sciences*, 48, 15–20.
43. Zohdi, T. I. (2010). On the dynamics of charged electromagnetic particulate jets. *Archieves of Computational Methods in Engineering*, 17(2), 109–135.
44. Zohdi, T. I. (2011). Dynamics of clusters of charged particulates in electromagnetic fields. *International Journal of Numerical Methods in Engineering*, 85, 1140–1159.
45. Zohdi, T. I., & Wriggers, P. (2008). *Introduction to computational micromechanics*, Second reprinting. New York: Springer.

Dynamics of Charged Particulate Systems

Modeling, Theory and Computation

Zohdi, T.I.

2012, XI, 115 p. 47 illus., 9 illus. in color., Softcover

ISBN: 978-3-642-28518-9